

## Composition of Tourmalines from Hajiabad and Dehghah area, SE Boroujerd

Amir Ali Tabbakh Shabani<sup>1\*</sup>, Reza Zarei Sahamieh<sup>2</sup>, Zohre Keshavarz<sup>1</sup>

<sup>1</sup> Faculty of Earth Sciences, Kharazmi University, Tehran, Iran

<sup>2</sup> Department of Geology, Lorestan University, Khorramabad, Iran

\*Corresponding author, e-mail: aatshabani@gmail.com

(received: 22/06/2012 ; accepted: 26/11/2013)

### Abstract

Tourmaline can be found as an accessory mineral in a variety of rocks including leucogranite, pegmatite, quartz veins, and metamorphic country rocks in Hajiabad-Dehghah area in SE of Boroujerd city. Tourmaline in pegmatites is coarse-grained, subhedral to euhedral, and displays strong to moderate pleochroic blue rimmed by olive green. In contrast, tourmalines from leucogranite, quartz-veins, and hornfels schist are very fine- to medium-grained, mainly subhedral to euhedral and in some cases zoned. They are strongly pleochroic with generally bluish green to brownish olive colors. The replacement of some feldspar grains by tourmaline forming skeletal texture is also common in leucogranite. The tourmaline in pegmatite is Fe-rich schorl ( $Fe/(Fe + Mg) = 0.86-0.95$ ), whereas those in leucogranite, quartz veins and hornfels schist are of schorl-dravite composition ( $Fe/(Fe + Mg) = 0.31-0.61$ ). Tourmalines in all these rock types are aluminous, alkali-rich, with Na being the dominant alkali element present, and they have small amounts of X-site vacancy. However, the distinct dissimilarity is the Zn contents of pegmatite schorl tourmaline (on average 0.02 apfu), which are noticeably lower than those of tourmalines of schorl-dravite composition (on average 0.13 apfu). The dominant variability in composition of the studied tourmalines seems to be controlled mainly by the alkali-deficient  $AlO_{0.5}Mg_{0.5}(OH)_1$  and proton-deficient  $\square AlNa_{-1}Mg_{-1}$  exchange substitutions. Tourmaline grains from pegmatite have the chemical features of tourmalines from Li-poor granitoids and associated pegmatites and aplites, whereas those from leucogranite, quartz-veins and hornfels schist possess the chemical characteristics of tourmalines from Ca-poor metapelites, metapsammites, and quartz-tourmaline rocks.

**Keywords:** Broujerd, granite, pegmatite, Sanandaj-Sirjan zone, Tourmaline

### Introduction

Tourmaline is a complex borosilicate mineral commonly found as an accessory phase in a variety of sedimentary, igneous, and metamorphic rocks, as well as hydrothermal rocks. This diversity is due to the ability of the tourmaline structure to accommodate a large variety of cations in terms of size and charge in a number of nonequivalent sites, which in turn leads to 14 recognized mineral species; of which the most common ones are elbaite, schorl, and dravite (Hawthorne & Henry, 1999). Because of its resistance to alteration and weathering, tourmaline preserves its primary composition; therefore, it is considered as an excellent petrogenetic indicator (Henry & Guidotti, 1985, Henry & Dutrow, 1996).

The present study is an attempt to describe tourmalines from different rock types from Hajiabad-Dehghah area in the south-east of Boroujerd city, compare the textural features and chemical compositions, assess the extent to which tourmaline chemistry reflects the bulk composition of the host-rocks, and discuss its petrogenetic significance. The analytical techniques used are electron microprobe analyses (EMPA) for major element and inductively coupled plasma atomic

emission spectrometry (ICP-AES) for trace element contents of tourmaline.

### Geological setting

The study area is located in the northern part of the Sanandaj-Sirjan metamorphic-magmatic zone, west-Central Iran (Fig. 1). The Sanandaj-Sirjan zone, trending NW-SE with a length of about 1500 km and a width of 150-250 km, is a part of Zagros orogeny; located between Urumieh-Dokhtar magmatic zone and Zagros fold thrust zone (Alavi, 1994). It consists of metamorphic and complexly deformed rocks associated with abundant deformed and undeformed plutons as well as Mesozoic volcanic rocks. The development of the zone resulted from the opening and closure of the Neotethys Ocean between Eurasia and Arabia (Mohajjel *et al.*, 2003; Ghasemi & Talbot, 2006). The plutonic suites cropping out in the NW of the zone are considered as arc-related calc-alkaline rocks generated during the Mesozoic, due to the subduction of Neotethys beneath the Iranian plate (Ahmadi-Khalaji *et al.*, 2007). Boroujerd Granitoid Complex (BGC), one of the suites occurring within this zone, is a NW-SE elongate body covering an outcrop area of about 200 km<sup>2</sup>. The complex

comprises three main units: quartz diorite, granodiorite, and monzogranite (Fig. 1). Zircon U-Pb age determination of the three plutonic units ranges from 169 to 173 Ma, corresponding to Middle Cimmerian orogeny (Ahmadi-Khalaji, 2006). The detailed study on geochronology,

geology, and geochemistry of the BGC by Khalaji et al., (2007) reveals that the granitoids are metaluminous to slightly peraluminous; high-K calc-alkaline rocks of I-type related to the mid-Jurassic subduction setting.

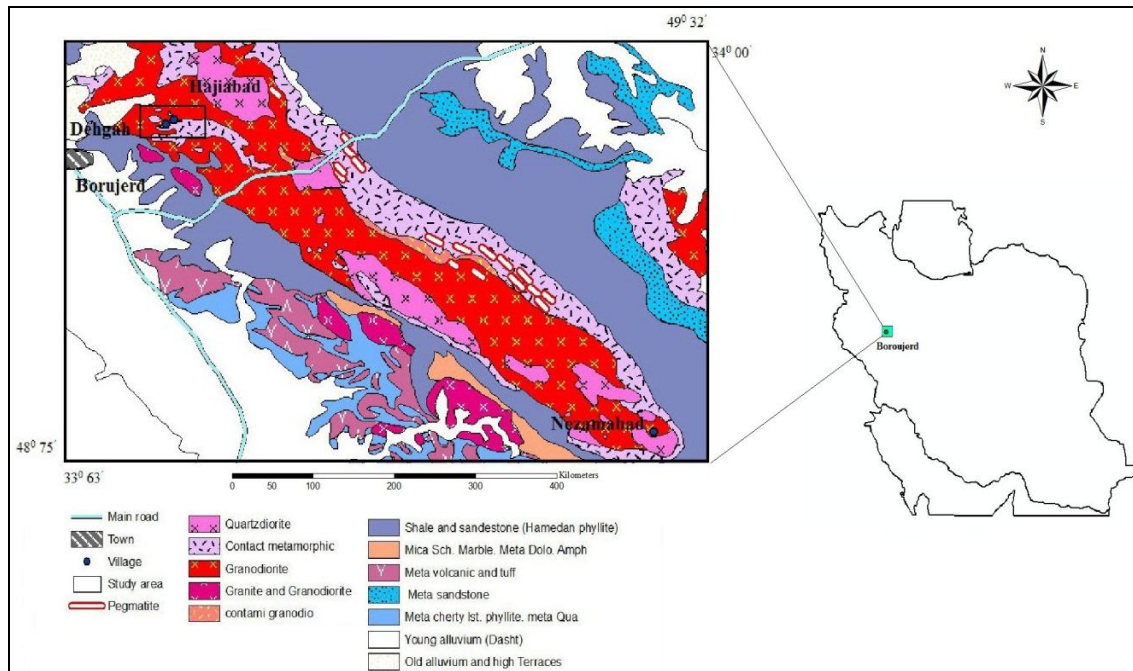


Figure 1: Regional geological map of the Boroujerd Granitoid Complex in the west of Iran (after Khalaji et al., 2007), with the box outlining the Hajiabad-Dehghah study area in the NW end of the complex.

The study area, located in the south east of Broujerd city in an area restricted between Hajiabad and Dehghah villages, is a small part of the northern portion of BGC that consists of a medium-grained leucocratic granite and granitic pegmatite surrounded by hornfels schists and Jurassic phyllites (Fig. 1). The leucogranite is the youngest intrusive phase that evolved from BCG. Pegmatite and quartz-tourmaline veins intersect the leucogranite and Jurassic phyllites. In addition to occurring in pegmatite as coarse-grained prismatic black crystals, the tourmalines within the leucogranite occur generally as clusters and patches, in quartz veins; crosscutting the leucogranite, as an assemblage of quartz and opaque minerals and in the country rocks of contact zones surrounding both leucogranite and pegmatite as very small prismatic crystals parallel to the schistosity.

#### *Tourmaline Occurrences and Petrography*

Four modes of tourmaline occurrence are identified in the study area based on the textural differences

observed among the tourmalines from the various rock types: (1) coarse-grained prismatic crystals of tourmaline (up to 2.5 cm in length) in pegmatite accompanied mainly by large crystals of quartz, feldspars, and muscovite, (2) clusters and patches of tourmaline in leucogranitic rocks, (3) fine-grained crystals of tourmaline in quartz veins, and (4) very fine grained crystals of tourmaline in hornfels schist from metamorphic halo of leucogranite.

*Pegmatite:* Quartz, plagioclase, microcline, minor muscovite, and tourmaline constitute the pegmatite. In this rock, euhedral to subhedral tourmalines form skeletal crystals; the cores of which consist of quartz and microcline. This texture probably formed through early nucleation and the growth of tourmaline, followed by simultaneous crystallization of quartz and microcline.

In thin section, quartz is anhedral, polycrystalline and shows wavy extinction. Tourmaline crystals are color-zoned, and their cores are homogeneous and surrounded by narrow rims. Pleochroism changes from light blue to dark blue in the core to olive-brown in a narrow zone surrounding the core.

Tourmaline grains are usually segmented by cracks and filled with quartz and microcline. In some

cases, tourmaline is replaced by quartz (Fig 2a).

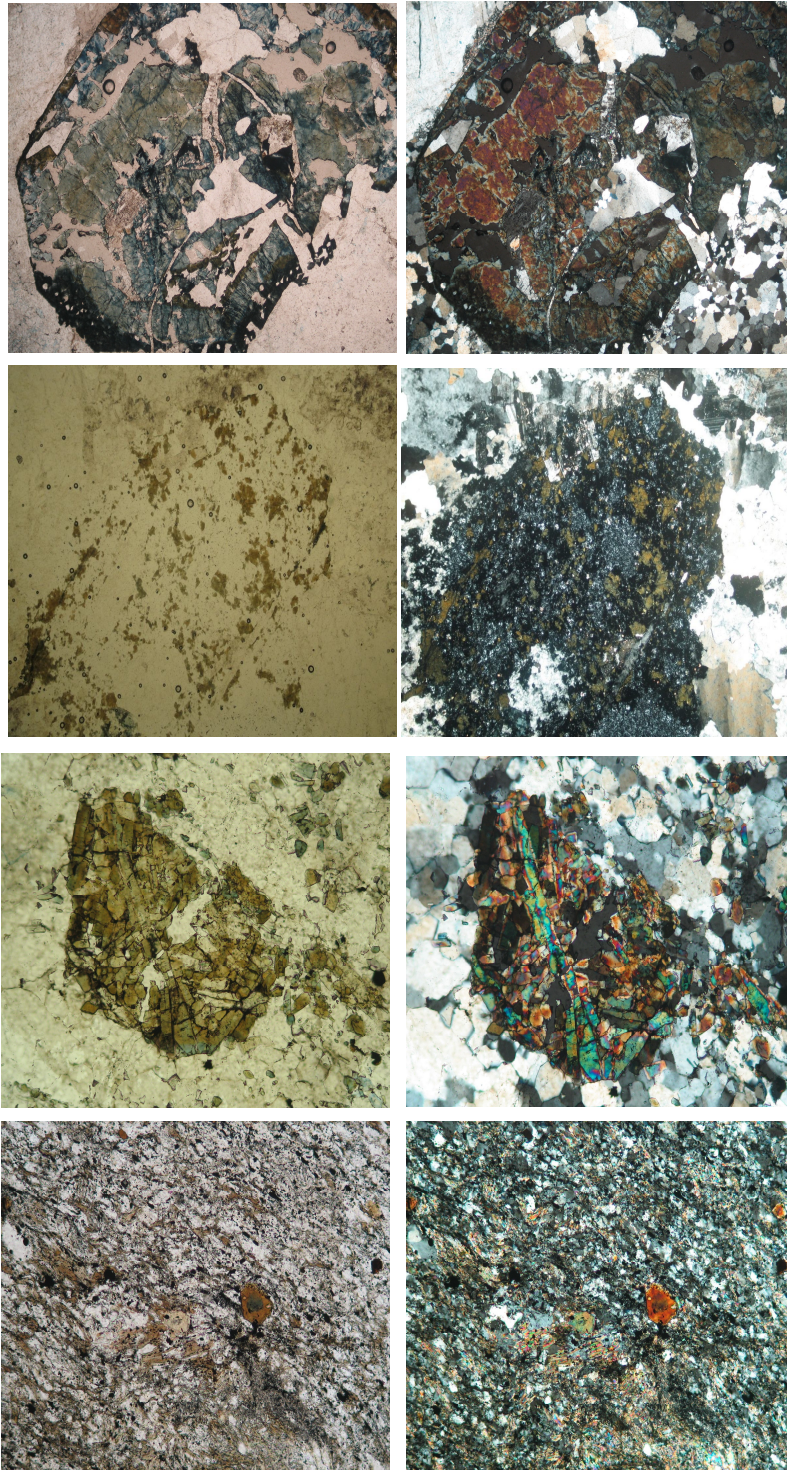


Figure 2: Photomicrographs showing different tourmaline occurrences in the studied samples from Hajiabad-Dehgah area in plane-polarized light (left) and crossed-polarized light (right): (a) Tourmaline cross-section in pegmatite. The euhedral zoned tourmaline has a core and a rim. Some parts of the tourmaline are replaced by quartz. (b) Skeletal tourmaline in the leucogranite showing partial replacement of a sericitized feldspar grain. (c) Clusters of fine-grained tourmalines in a quartz-tourmaline vein. The bluish and brownish pleochroic patches indicate compositional zoning. (d) Tourmaline from a metapelitic schistose hornfels, cut perpendicular to the c axis. An olive brown rim surrounds the light blue core.

**Leucogranite:** The leucogranite is mainly medium grained, light in color and has a simple mineralogy comprising plagioclase, microcline, quartz, and muscovite. Skeletal or incompletely formed crystals of tourmaline occur exclusively within some of the euhedral and subhedral feldspar grains, indicating the replacement of feldspar by tourmaline (Fig. 2b). Based on this textural relationship, tourmaline within the leucogranite is regarded as a metasomatic mineral.

**Quartz veins:** The quartz - tourmaline veins, ranging in thickness from few centimeters to almost one meter, crosscut the granitic rocks and can also be found along the boundary between leucogranite and contact metamorphic aureole. Mineralogy of quartz- tourmaline veins is simple and consists mainly of quartz and tourmaline as well as small amounts of feldspars and opaque minerals. The aggregates of fine-grained prismatic crystals of tourmaline occurring in quartz veins do not exceed 15% by volume. Therefore, the term tourmalinite veins cannot be used as defined by Nicholson (1980), Slack (1982), and Fortey and Cooper (1986). Most of the grains display a light blue-green core that changes into a darker olive brown around the rim.

Optically irregular zoning occurs as patchy domains of blue green in brownish green regions. Some well-defined cores have outer zones showing an irregular distribution of coloring (Fig. 2c). Tourmaline grains may be unzoned, irregularly zoned, or have two sharply defined zones. A light bluish green core and a deep olive green rim characterize color zonation.

**Hornfels Schist:** Tourmaline is very fine grained (<1 mm) and is found in the metamorphic country rocks of greenschist facies at the contact of granite. Figure 2d shows an image of a thin section cut to the schistosity of the rock displaying lepidogranoblastic texture. As it can be seen in Figure 2d, prismatic cross sections of some tourmaline crystals display two optically distinct growth zones, developed concentrically about the c axis and nearly parallel to the crystal faces. A greenish blue core gives way to a brownish green rim. Optically unzoned crystals are also common (Fig.2d).

### Material and Methods

For the purpose of this study, a total of 30 samples were collected from different rock types in the study area. Standard petrographic thin sections were

prepared from all rock samples and studied by polarizing microscope. Subsequently, 8 samples were selected (three samples of leucogranite, three samples of quartz vein, one sample of pegmatite, and one sample of hornfels schist), and polished thin sections were prepared for electron microprobe analysis. A total of 65-point analyses were determined on tourmalines from the selected samples. In general, a minimum of three analyses were taken per grain.

Tourmaline analyses were obtained by wavelength-dispersive X-ray spectrometry on polished thin sections, prepared from each rock sample for 12 elements using Cameca SX-100 electron microprobe at the Iran Mineral Processing Research Center. Typical beam operating conditions were 15 kV and probe current 20 nA. Natural oxide and silicate mineral reference materials were used for calibration. Analytical errors on all analyses were 1% relative for major elements and 5% relative for minor elements.

Mineral recalculation, classification, and various plots of tourmaline were made using WinClastour program, presented by Yavuz *et al.*, (2006). Structural formulae were calculated on the basis of 31 oxygens, assuming stoichiometric amounts of H<sub>2</sub>O as (OH), i.e., OH + F = 4 atoms per formula unit (apfu). Because B and Li cannot be measured on the microprobe, B<sub>2</sub>O<sub>3</sub> concentrations were calculated stoichiometrically to 3 B per formula unit. The amount of Li assigned to the Y site corresponds to the ideal sum of the cations occupying the T + Z + Y sites (15 apfu) minus the sum of the cations occupying these sites, i.e., [Li = 15 - (T + Z + Y)]; assuming no vacancies in the octahedral sites (Henry & Dutrow, 1996). All Fe and Mn were assumed to be divalent, because crystal-structure studies have demonstrated that this is the most frequent valence state of Mn and Fe in tourmaline (Burns *et al.*, 1994, Bloodaxe *et al.*, 1999). The average composition of tourmaline grains from each rock type along with its structural formula is presented in Table (1).

To determine the contents of trace and rare earth elements (REE), the researchers separated tourmaline grains from 3 samples; excluding hornfels schist, because tourmaline separation from this sample was unsuccessful due to its low content. The procedures of separation are as follows: whole rock samples were crushed using both jaw crusher and pulverizer. The crushed samples were then sieved to obtain the size fraction between 45 and 60 mesh (350-250 μm). All samples were washed with water to remove dust. Magnetite was removed with a strong permanent

magnet, and the mafic and felsic grains were then separated using a Frantz magnetic separator. Further

purification was achieved using heavy liquids (methylene iodide, S.G. = 3.33).

Table 1: Average chemical compositions of tourmaline from pegmatite, leucogranite, quartz veins, and hornfels schist along with their structural formulae based on 31 (O, OH, F). The measured FeO is considered as Fe<sup>2+</sup>.

	pegmatite	leucogranite	quartz veins	hornfels
<b>mean of analyses</b>	10	23	25	7
SiO <sub>2</sub>	34.18	34.44	34.10	33.85
TiO <sub>2</sub>	0.82	1.15	1.25	0.79
Al <sub>2</sub> O <sub>3</sub>	33.91	33.02	34.05	32.93
Cr <sub>2</sub> O <sub>3</sub>	0.02	0.02	0.09	0.39
FeO*	13.88	9.23	7.30	9.44
MgO	0.82	4.53	5.33	5.03
CaO	0.14	0.39	0.77	0.59
MnO	0.10	0.06	0.02	0.00
ZnO	0.18	1.19	1.03	0.97
Na <sub>2</sub> O	1.73	1.80	1.67	1.92
K <sub>2</sub> O	0.04	0.05	0.03	0.07
F	0.42	0.27	0.19	0.43
H <sub>2</sub> O*	3.35	3.46	3.53	3.38
B <sub>2</sub> O <sub>3</sub> *	10.28	10.41	10.50	10.38
Li <sub>2</sub> O*	0.22	0.08	0.13	0.02
O=F	0.18	0.11	0.08	0.18
<b>Total*</b>	99.90	99.99	99.92	100.01
<b>structural formula based on 31 anions (O, OH, F)</b>				
Si	5.78	5.75	5.65	5.67
AlT	0.22	0.25	0.35	0.33
ΣT-site	6.00	6.00	6.00	6.00
B	3.00	3.00	3.00	3.00
AlZ	6.00	6.00	6.00	6.00
AlY	0.54	0.25	0.29	0.17
Ti	0.10	0.14	0.16	0.10
Cr	0.00	0.00	0.01	0.05
Mg	0.21	1.13	1.32	1.26
Mn	0.01	0.01	0.00	0.00
Fe <sup>2+</sup>	1.96	1.29	1.01	1.32
Zn	0.02	0.15	0.13	0.12
Li*	0.15	0.05	0.09	0.01
ΣY-site	3.00	3.02	3.00	3.03
Ca	0.03	0.07	0.14	0.11
Na	0.57	0.58	0.54	0.63
K	0.01	0.01	0.01	0.02
ΣX-site	0.60	0.66	0.68	0.75
vacancy	0.40	0.34	0.32	0.25
OH	3.78	3.86	3.90	3.77
F	0.22	0.14	0.10	0.23
Mg/Fe	0.10	0.87	1.30	0.95
Fe/Fe+Mg	0.91	0.53	0.43	0.51
<b>FeO* as total iron</b>				
* calculated from stoichiometry				

The separates were then examined under a binocular microscope to remove contaminated grains by handpicking, until the concentrates appeared to be at least 99% pure. Then, they were ground by hand in

an agate mortar under acetone to obtain a 200 mesh powdered samples. Finally, trace and REE analyses of the separates were carried out by ICP-AES at the Geological Survey of Iran laboratories.

## Discussion

### Mineral Chemistry

The average chemical composition of the study tourmalines from various rock types were determined by electron microprobe along with their structural formulae calculated based on general formula of tourmaline  $XY_3Z_6T_6O_{18}(BO_3)_3V_3W$ , (Hawthorne & Henry, 1999; Hawthorne, 2002), where X = Ca, Na, K, □ (vacancy); Y =  $Li^{+1}$ ,  $Fe^{2+}$ ,  $Mg^{2+}$ ,  $Mn^{2+}$ ,  $Zn^{2+}$ ,  $Al^{3+}$ ,  $Cr^{3+}$ ,  $V^{3+}$ ,  $Fe^{3+}$ ,  $Ti^{4+}$ , □ (vacancy); Z =  $Mg^{2+}$ ,  $Al^{3+}$ ,  $Fe^{3+}$ ,  $V^{3+}$ ,  $Cr^{3+}$ ; T = Si, Al, (B); B = B, □ (vacancy); V = OH, O; W = OH, F, O (Table 1).

Calculations of site occupancies show that in almost all samples of our tourmaline Si is insufficient to fill the tetrahedral sites; therefore, some Al is required to fill the T sites (Table 1). The six octahedral Z sites are fully occupied by Al and the three octahedral Y sites, slightly larger and distorted, are occupied by different cations including Al, Ti, Cr, Mg, Mn,  $Fe^{2+}$ , Zn, and Li. In fact, the main compositional variable of tourmaline is the occupancy of the Y site. The sum of T + Z + Y cations is 15, indicating no vacancies in the T, Z, and Y sites, and it is consistent with the tourmaline ideal formula. The occupancy of the X site by Ca, Na, and K ranges from 0.33 to 0.76 apfu compared to the ideal value of 1.0 apfu for tourmalines of the schorl-dravite solid solution. This implies the presence of vacancies in the X-site ranging from 0.67 to 0.24. The X-site vacancy is the smallest one in hornfels schist tourmaline and the largest in the pegmatite one (Table 1). In all of the studied samples, Na is dominant over Ca and K, at the X site. The Ca contents are low with the range from 0.01 to 0.19 apfu.

The amount of  $B_2O_3$  necessary to produce three B cations in the structural formula was calculated using stoichiometry. The triangular B site is occupied exclusively by B (Table 1).

There is a major variation in Fe content (1.01–1.96 apfu), whereas Al varies slightly between 6.50 and 6.76 apfu. In all cases, FeO contents are greater than MgO ones (Table 1).

Minor elements detected in the studied tourmalines are K, Mn, Ca, Cr, and Zn; among which Zn displays the highest values, reaching on average to 0.18, 1.19, 1.03, and 0.97 wt% in pegmatite, leucogranite, quartz veins, and hornfels schist, respectively (Table 1).

The classification and compositional details are best revealed by plotting the results of electron

microprobe analyses on a series of compositional diagrams (Figs. 3–9). On the ternary (Ca, X-site vacancy, Na + K) diagram of Hawthorne and Henry (1999), except for a few samples, the majority of samples plot in the alkali group field with minor X-site vacancies and Ca substitution for Na (Fig. 3).

The calculated Al in the structural formulae is greater than 6 apfu. The excess of Al (up to 6.61 apfu), compared with the theoretical value of 6 in ideal schorl and dravite, classifies our samples as aluminous tourmalines.  $Al^{3+}$  occupancy is significant in the Y site of tourmalines from various rocks: in leucogranite it ranges from 0.06 to 0.50 with a mean value of 0.25 (apfu); it is relatively high in pegmatite from 0.38 to 0.67, on average 0.54 (apfu); in quartz tourmaline veins from 0.01 to 0.51, on average 0.29 (apfu); and relatively less in hornfels schist from 0.05 to 0.27 with a mean value of 0.17 apfu (Table 1).

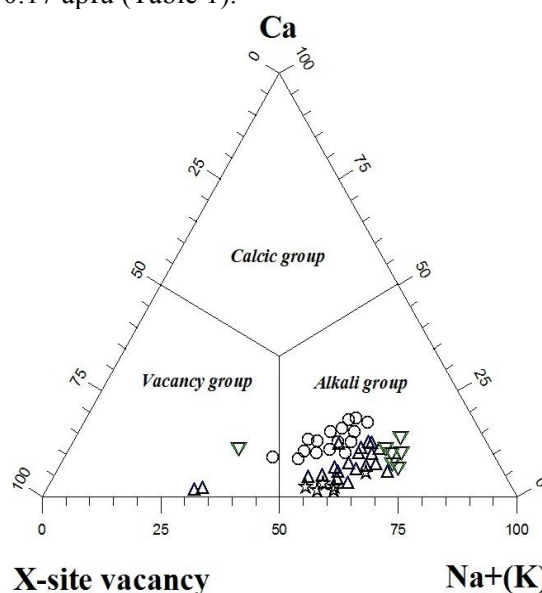


Figure 3: Classification diagram based on X-site occupancy, Ca, and Na+K contents of tourmalines after Hawthorne and Henry (1999), showing that the majority of samples plot in the alkali group tourmalines.

Tourmalines from pegmatite leucogranite quartz veins hornfels:



The best diagram for classification of the tourmaline species is established by Hawthorne and Henry (1999) in which X-vacancy/(X-vacancy + Na) is plotted versus  $Mg/(Mg + Fe)$ . On this diagram, most of the tourmaline specimens fall within the schorl and dravite, except a small number in foitite fields (Fig. 4). As it can be seen in Figure 4, tourmalines from pegmatite are

compositionally distinctive, i.e., they have higher concentrations of Fe and lower concentrations of Mg ( $Mg/Fe=0.1$  on average) than those found in the leucogranite and quartz tourmaline veins and hornfels schist (the mean  $Mg/Fe$  ratios of tourmalines from these rocks are 0.87, 1.30 and 0.95, respectively) (Table 1). The tourmalines from quartz veins are slightly dravitic with respect to the rest, which are intermediate in composition between dravite and schorl end-members, with a slight tendency toward the schorl end-member (Fig. 4). Also note the lack of discrimination between the composition of tourmalines from leucogranite and hornfels schist (Fig. 4).

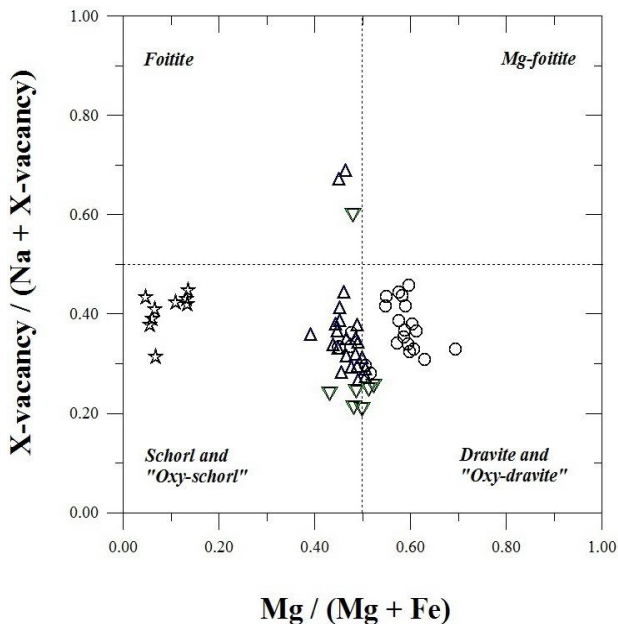


Figure 4: Compositions of Hajiabad-Dehgah tourmalines plotted in terms of X- vacancy /Na+ X- vacancy versus Mg/ (Mg+ Fe). End-member compositions of foitite, magnesio-foitite, schorl, oxy-schorl, and dravite, oxy dravite plot at the corners of the diagram. Note pegmatite hosted tourmalines are schorl; however, tourmalines from leucogranite, quartz veins, and hornfels schist are classified as intermediate schorl-dravite composition and a few as foitite.

On the Mg versus Fe diagram of London and Manning (1995), tourmaline defines a compositional trend parallel to the line  $\Sigma(Fe+Mg)=3$  that corresponds to the dravite-schorl exchange vector  $FeMg_{-1}$  (Fig. 5). There is, however, a systematic departure toward alkali-deficient tourmaline and oxy-tourmaline, which is due to Al substitution in the Y-site (R2). Henry and Dutrow (1990) have shown that substitution of  $Al^{3+}$  for divalent cations such as  $Mg^{2+}$  and  $Fe^{2+}$  in Y site is charge-compensated by deficit of alkalis and proton

in other structural sites of tourmaline according to the  $AlOMg_{-1}(OH)_{-1}$  and  $\square AlNa_{-1}Mg_{-1}$  exchange vectors.

On the diagram of London and Manning (1995), the schorl-dravite composition plots at  $Z=6$  and  $X+Y=4$ . Comparing with schorl-dravite, our compositional data are plotted in terms of the cation groups, i.e., R3 versus  $R1 + R2$  where  $R1 = (Na+Ca)$ ,  $R2 = (Fe+Mg)$ ,  $R3 = (Al+1.33Ti)$ . R1, R2 and R3 correspond to X, Y and Z sites of the tourmaline formula, respectively. As it can be seen in Figure 6, all of the tourmalines fall on or close to the exchange vector labeled proton deficient ( $\square AlNa_{-1}Mg_{-1}$ ), implying that alkali deficient substitution ( $AlOMg_{-1}(OH)_{-1}$ ) has been less effective than the proton deficient one on the composition of the study tourmalines. This suggests that crystallization of tourmaline was mainly buffered by alkalis instead of  $H_2O$ . In fact,  $H_2O$ -rich systems favor alkali-defect substitution (Gallagher, 1988).

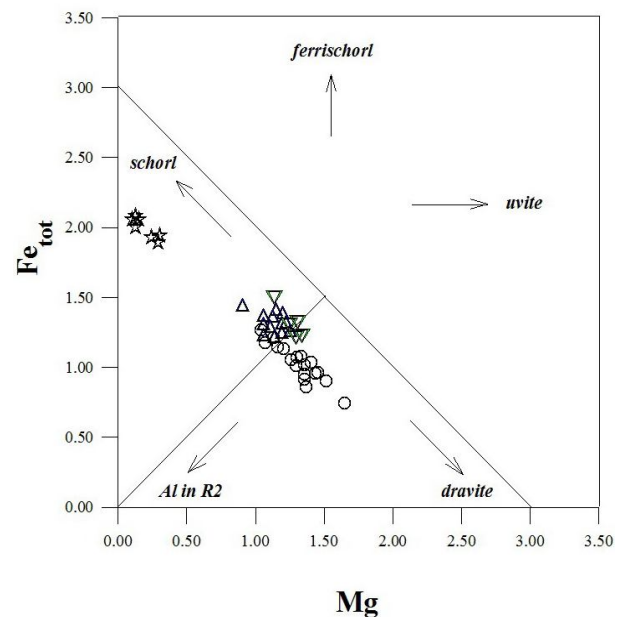


Figure 5: Plot of concentration of Fe versus that of Mg in tourmalines from Hajiabad-Dehgah area. Values are expressed in atoms per formula unit.

On the Al-Fe-Mg and Ca-Fe-Mg diagrams of Henry and Guidotti (1985), which show the relationship between tourmaline composition and the host rock type, tourmaline compositions from pegmatite exclusively plot in field 2, corresponding to tourmaline from Li-poor granitic rocks and associated pegmatites and aplites. And, those from leucogranite, quartz veins, and hornfels schist plot

in field 4, corresponding to Ca-poor metapelites, metapsammites and quartz-tourmaline rocks (Fig. 7). As it can be seen in Figure 7b, tourmalines plot in field 4 is above the schorl–dravite line with  $(\text{Fe} + \text{Mg}) < 3$  suggesting yet again insignificant uvite component in these minerals. In fact, the study tourmalines have some insignificant degree of uvite component with a range value of Ca from 0.03 to 0.14 apfu (Table 1).

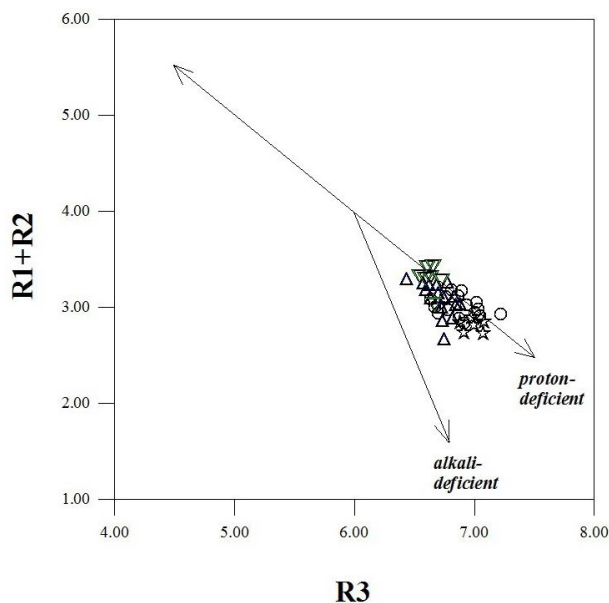


Figure 6: Compositional variations in tourmalines from Hajiabad-Dehgah area are shown in relation to common substitution mechanisms in tourmalines. The diagram after Manning (1982) shows that Al contents beyond 6.0 cations apfu are charge-balanced by vacancies in the X-site. The R1 variable is  $\text{Ca} + \text{Na}$ , the R2 variable is  $\text{Fe} + \text{Mg} + \text{Mn}$ , and the R3 variable is  $\text{Al} + 1.33\text{Ti}$ . The variations can be related to alkali defect and proton-loss substitutions in tourmaline. The vectors represent the possible exchange operator that could have operated in these tourmalines.

#### Rare-earth Elements

The results of ICP-AES analyses of REE and some trace elements for the three tourmaline sample separates are presented in Table 2. The total REE contents of tourmaline are largely different; 30 ppm in pegmatite, 83 ppm in quartz veins, and 460 ppm in leucogranite (Table 2). For comparison, chondrite normalized REE patterns of the tourmalines are represented in Figure 8. The REE pattern of leucogranite tourmaline resembles that of the quartz vein tourmaline, which may imply contribution from very similar hydrothermal fluids. Tourmaline from the quartz vein and tourmaline from the leucogranite show fractionated chondrite-normalized patterns ( $\text{LaN}/\text{YbN} = 59.26$  and  $9.93$ ,

respectively), and both have relatively higher light REE and lower heavy REE contents (Fig. 8).

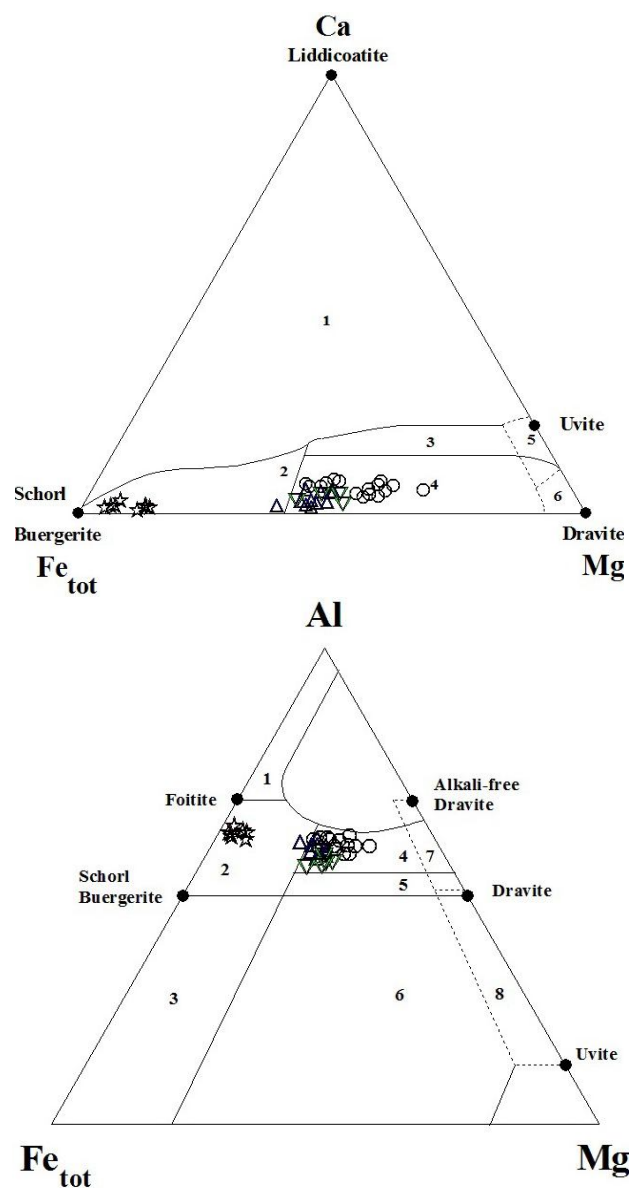


Figure 7: Discrimination diagrams for tourmaline from different rocks based on the Ca-Fe-Mg and Al-Fe-Mg diagrams (in molar proportions) for Hajiabad-Dehgah tourmalines with fields after Henry and Guidotti (1985) 1: Li-rich granitic pegmatites and aplites, 2: Li-poor granitic rocks and associated pegmatites and aplites, 3: Fe-rich quartz-tourmaline (hydrothermally altered granites), 4: metapelites and metapsammites coexisting with an Al-saturating phase, 5: metapelites and metapsammites not coexisting with an Al-saturating phase, 6: Fe-rich quartz-tourmaline rocks, calc-silicate rocks, and metapelites, 7: low-Ca meta-ultramafic and Cr, V-rich metasedimentary rocks, and 8: metacarbonate and metapyroxenites, 9: Ca-rich metapelites, metapsammites, and calc-silicate rocks, 10: Ca-poor metapelites and metapsammites and quartz-tourmaline rocks, 11: metacarbonates 12: meta-ultramafic rocks.

Table 2: Selected trace element concentrations in terms of ppm from representative tourmaline samples of pegmatite, leucogranite, quartz veins from Hajiabad-Dehgah area determined by ICP-AES.

samples	pegmatite	leucogranite	quartz- vein
Ba	23.2	71.5	119.8
Be	0.3	0.8	2.5
Co	27.0	24.8	36.4
Cr	0.5	96.9	89.0
Cs	8.3	4.5	3.9
Cu	516.0	20.5	14.4
Ga	39.4	32.1	28.7
Ge	2.2	1.1	0.8
Hf	14.5	7.9	6.2
Mo	1.2	0.7	0.8
Nb	2.9	27.2	14.0
Ni	8.3	55.3	57.3
P	206.4	947.6	536.4
Pb	64.0	17.9	39.0
Rb	2.8	16.1	11.2
Sc	11.0	14.3	12.7
Sn	4.2	1.8	2.0
Sr	11.0	63.0	44.6
Ta	6.3	2.1	0.7
Th	34.3	14.2	14.5
Tm	1.6	0.7	0.8
U	7.2	3.3	2.7
V	19.1	56.5	164.0
W	1.6	1.2	0.5
Y	3.6	11.3	2.4
Zn	166.0	278.0	85.3
Zr	12.0	29.0	14.9
La	0.3	114.0	19.1
Ce	0.6	216.0	41.9
Pr	1.0	12.8	5.7
Nd	0.6	78.1	8.4
Sm	0.5	18.9	3.1
Eu	0.0	0.6	0.1
Gd	4.7	8.3	1.7
Tb	1.4	0.6	0.4
Dy	0.1	7.6	0.1
Ho	0.7	1.1	0.2
Er	0.5	2.0	1.1
Tm	1.6	0.7	0.8
Yb	1.3	0.8	0.6
Lu	0.7	0.2	0.1
ΣREE	29.9	459.8	83.4

In contrast, the pegmatite tourmaline shows a weakly fractionated pattern with a chondrite-normalized value of  $LaN/YbN = 0.16$ , and is moderately enriched in light REE, except Pr, and poorly depleted in heavy REE. As can be seen in Figure 8, all tourmaline REE patterns are characterized by negative Eu anomaly.

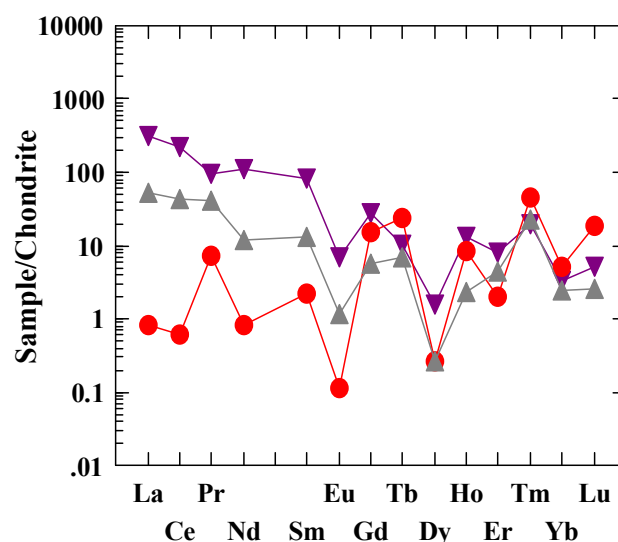


Figure 8: REE concentrations of tourmalines from Hajiabad-Dehgah area normalized to Chondrite C1 (Sun & McDonough, 1989).

Pegmatite: ● leucogranite: ▼ quartz vein: ▲

Tourmalines from leucogranite have higher concentrations of the total trace elements than those of the quartz veins and pegmatite. Chondrite-normalized patterns of the selected trace elements from the tourmaline in quartz-tourmaline veins, tourmaline from the leucogranite, and tourmaline from pegmatite are shown in Figure 8. The pattern of leucogranite tourmaline resembles that of the quartz tourmaline veins; however, the plot shows a slightly different pattern for pegmatite tourmaline, especially for transition elements Cr and Ni (Fig. 9). This difference between pegmatite tourmaline and the other two is consistent with its occurrence, mineralogy features, and distinct composition as described earlier. On the other hand, similarities seen in patterns of tourmalines from leucogranite and quartz veins may imply contribution from similar sources, i.e., magmatic-hydrothermal fluids are responsible for the vast tourmalinization in the study area.

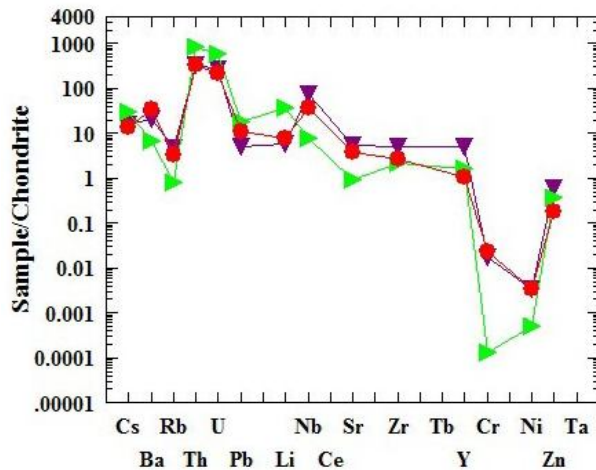


Figure 9: Concentrations of selected trace elements of tourmalines from Hajiabad-Dehgah area normalized to Chondrite C1 (Sun & McDonough, 1989).

Pegmatite: ▲ leucogranite: ▼ quartz vein: ●

## Discussion

It is very likely that the tourmalines with schorl composition, characterized by higher concentrations of Fe, are of magmatic origin as they are associated with the pegmatite veins. This type of tourmaline is crystallized directly from the magma and here is referred to as primary tourmaline. This can be further confirmed by the Al-Fe-Mg and Ca-Fe-Mg diagrams of Henry and Guidotti (1985), which show the relationship between tourmaline composition and the host rock type on which tourmaline compositions from pegmatite exclusively plot in field 2; which in turn corresponds to tourmaline from Li-poor granitic rocks and associated pegmatites and aplites (Fig.7).

As shown above, the tourmalines from leucogranite, quartz-tourmaline veins, and hornfels schist have chemical similarities despite their different textural characteristics. The composition of tourmalines from these rocks is intermediate schorl-dravite end members with  $Fe/Fe+Mg \approx 0.5$  (Table 1). Foit and Rosenberg (1977) reported that both alkali-defect and dehydroxylation substitutions can produce the intermediate composition between schorl-dravite end-members.

What seems apparently inconsistent here is that tourmaline from leucogranite does not display compositions typical of Li-poor granitoids and their associated pegmatites and aplites (field 2 in Fig.7); conversely, its composition corresponds to tourmaline of Ca-poor metapelites, metapsammites, and quartz-tourmaline rocks. This may imply that

tourmaline in leucogranite could not have crystallized from magma and hence was presumably formed from a hydrothermal origin. In fact, the present study's leucogranite, which is mainly composed of quartz and feldspar, is mineralogically similar to the metapsammites, which are metamorphosed feldspathic sandstones. Therefore, it seems that inconsistency of the relationship between tourmaline composition and its host rock can be justified in this way (Fig. 7).

Tourmaline is a relatively common mineral in peraluminous granites and starts to crystallize when the aluminum saturation index (ASI) of magma reaches a value between 1.3 and 1.4,  $B_2O_3$  is concentrated to a value of  $\sim 2$  wt%, and adequate Fe and Mg are available in the melt (London & Manning, 1995, London *et al.*, 1996, Wolf & London, 1997). Tourmaline is unstable in peralkaline, metaluminous, and peraluminous, and it melts with an ASI less than 1.2 (Wolf & London 1997). Consequently, the studied leucogranite, composed mainly of feldspar and quartz (barely peraluminous) with no or relatively very low Fe, Mg, and B contents, does not favor direct crystallization of tourmaline. This can be confirmed by the occurrence of incompletely formed crystals of tourmaline within feldspar grains of leucogranite, i.e., tourmaline was obviously developed at the expense of plagioclase, implying a boron-rich hydrothermal origin rather than a magmatic one.

The origin or source of the boron will be left unanswered in this study and its isotopic determinations will be a subject for future studies. However, the most recent studies on tourmalines in the south-eastern part of the Borojerd granitoid complex at Nezamabad region (Fig. 1) by Nekouvaght and Bazargani (2009) and Esmaily *et al.*, (2009) have shown that chemical and boron isotopic composition of tourmalines from quartz diorite and quartz-tourmaline veins indicate that these tourmalines are of intermediate schorl-dravite composition and their  $\delta^{11}B$  values, which are in the range of clastic metasedimentary and metavolcanic rocks, confirm a boron source derived from mostly metasedimentary rocks. In addition, Masoudi (1997) has also demonstrated the tourmaline crystals in the aureoles of Borojerd granitoid complex derived from the metamorphic source. Based on the obtained  $\delta^{11}B$  values, Haghazari (2007) has concluded that Borojerd granitoid magma could be considered as a partial source of boron due to its incompatible behavior through

magma crystallization leading to accumulation in more evolved fluids. The mixture of these granitic hydrothermal fluids with those derived from dehydration reactions and leaching of contact metasediments has been responsible for the vast tourmalinization of the area. Likewise, we believe that the same scenario must have worked in Dehgah and Hajiabad area of the north-western part of the BGC leading to similar tourmaline compositions.

The presence of magmatic tourmaline in pegmatite, evolved from Boroujerd granitoids, suggests that the magmas of BGC could be considered as the source of boron due to its incompatible behavior through magma crystallization leading to accumulation in more evolved fluids. Therefore, the mixture of these granitic fluids with those derived from dehydration reactions and leaching of contact metasediments during hydrothermal circulation associated with magmas of BGC must have been responsible for the vast tourmalinization of the area.

However, because leucogranite is composed essentially of feldspar and quartz with minor muscovite, which is mineralogically similar to psammitic rocks, it does not contain enough Al, Mg, and Fe to form tourmaline through reaction of boron-rich fluids with feldspar. Hence, these fluids must have carried and supplied the necessary cations from probably adjacent surrounding metamorphic rocks into the leucogranite. This argument seems consistent with the tourmaline major element compositions plotting in the field of metasedimentary rocks in the discrimination diagrams of Henry and Guidotti (1985) (Fig. 7).

The presence of tourmaline in the quartz veins suggests high concentrations of boron in the hydrous silica-bearing fluids. Boron could be released into the circulating fluids from contact metasedimentary rocks by an increase in the temperature, supplied by magma. Possible sources of these fluids include the host metasedimentary rocks and magmatic or postmagmatic fluids. In any case, it is inferred that the B-enriched fluids reacted with the host rocks along zones of structural weakness or narrow fractures and through inter- or intragranular pore-space. According to London and Manning (1995), quartz-tourmaline veins within granitic bodies reflect a hydrothermal origin rather than a magmatic origin.

Our microprobe data show that the composition of tourmalines in leucogranite overlaps with the composition of tourmalines in hornfels schist

(Fig.3). On the other hand, comparison of our data from hornfels schist with compositional fields of tourmalines with known origins (from Henry and Guidotti (1985) indicates that metapelites and metapsammities are most likely the protholith. Pelitic metasediments contain enough Al, Mg, Fe, Ca, and Na to form tourmaline through reaction with boron-rich fluids (Morgan & London, 1989; Fuchs & Lagache, 1994). Similarly, tourmaline is formed as a result of the metasomatic replacement of pelitic rocks by boron-rich hydrothermal fluids that were derived from both adjacent felsic magma and metamorphic rocks.

Raith *et al.*, (2004) demonstrated that REE concentrations and patterns of tourmalines are not controlled by hydrothermal fluids causing boron metasomatism; however, they are inherited from and controlled by host rock in which tourmaline is crystallized. However, the similar patterns of chondrite-normalized REE and the selected trace elements of both leucogranite and quartz vein tourmalines suggest that the trace elements might have partly contributed to the system by hydrothermal solutions (Klein & Beukes 1989). As explained earlier, both leucogranite and quartz vein hosted compositionally similar tourmalines and similar REE and trace element patterns, which imply a similar fluid source(s). A lower REE concentration together with the lowest negative Eu and higher positive Pr, Tm, and Lu anomalies of chondrite-normalized REE pattern of tourmaline from pegmatite shows a trend which is different from that of tourmalines in leucogranite and quartz vein, indicating a different crystallization environment.

### Conclusion

From the data presented, it can be concluded that the textural and chemical differences observed between tourmaline from the pegmatite and tourmalines from leucogranites, quartz veins, and hornfels schist suggest different origins. Tourmalines from pegmatite, showing limited chemical variation of schorl composition, are regarded as magmatic, whereas tourmalines from leucogranite, quartz veins, and contact metamorphic aureole, display intermediate schorl-dravite composition, as hydrothermal. The composition of tourmalines indicates the involvement of both alkali-deficient and proton-deficient substitutions, with the latter being more effective

**Acknowledgements**

The writers are grateful to anonymous referees for

their constructive comments and corrections that helped us to improve the manuscript.

**References**

- Alavi, M., 1994. Tectonics of the Zagros Orogenic belt of Iran: new data and interpretation. *Tectonophysics*, 229, 211-238.
- Bloodaxe, E.S., Hughes, J.M., Dyar, M.D., Grew, E.S., Guidotti, C.V., 1999. Linking structure and chemistry in the schorl–dravite series. *American Mineralogist*, 84: 922-928.
- Burns, P.C., Macdonald, D.J., Hawthorne, F.C., 1994. The crystal chemistry of manganese-bearing elbaite. *Canadian Mineralogist*, 32: 31-41.
- Esmaily, D., Trumbull, R.B., Haghaziar, M., Krienitz, M.S., and Wiedenbeck, M., 2009. Chemical and boron isotopic composition of hydrothermal tourmaline from scheelite-quartz veins at Nezamabad, western Iran. *European Journal of Mineralogy*, 21: 347-360.
- Foit, F. F., Rosenberge, P. E., 1977. Coupled substitution in the tourmaline group. *Contribution to Mineralogy and Petrology*, 62: 109-127.
- Fortey, N.J., Cooper, D.C., 1986. Tourmalinization in the Skiddaw Group around Crummock Water, English Lake District. *Mineralogical Magazine*, 50: 17-26.
- Fuchs, Y., Lagache, M., (1994) La transformation chlorite-tourmaline en milieu hydrothermal, exemples naturels et approche expérimentale. *C R Acad Sci Paris* 319:907- 913
- Gallagher, V., 1988. Coupled substitutions in schorl-dravite tourmaline: new evidence from SE Ireland. *Mineralogical Magazine*, 52: 637-650.
- Ghasemi, A., Talbot, C.J., 2006. A new tectonic scenario for the Sanandaj-Sirjan Zone (Iran). *Journal of Asian Earth Sciences*, 27: 683-693.
- Haghaziar, M., 2007. Petrogenesis and Nezam Abad Tungsten Mineralization in the South West of Boroujerd Granitoid Complex (West Iran). M.Sc. Thesis (in Persian), University of Tehran, Iran, 145 pages.
- Hawthorne, F.C., Henry, D.J., 1999. Classification of the minerals of the tourmaline group. *European Journal of Mineralogy*, 11: 201-215.
- Hawthorne, F.C., 2002. Bond-valence constraints on the chemical composition of tourmaline. *Canadian Mineralogist*, 40: 789-797.
- Henry, D.J., Guidotti, C.V., 1985. Tourmaline as a petrogenetic indicator mineral: an example from the staurolite grade metapelites of NW- Marine. *American Mineralogist*, 70: 1-15.
- Henry, D.J., Dutrow B.L., (1996) Metamorphic tourmaline and its petrologic applications. In: Grew Es, Anovitz LM (eds) Boron. *Mineralogy, Petrology and Geochemistry*. The Mineralogical Society of America, Washington DC, *Reviews in Mineralogy*, 33: 503-557.
- Henry, D.J., Dutrow, B., 1990. Evolution of tourmaline in metapelitic rocks: Diagenesis to melting. *Geological Society of America Abstracts with Programs*, 22: A125.
- Klein, C., Beukes, N.J. 1989. Geochemistry and sedimentology of a facies transition from limestone to iron-formation deposition in the Early Proterozoic Transvaal Supergroup, South Africa. *Econ. Geol.*, 84: 1733-1774.
- Khalaji, A.A., Esmaily, D., Valizadeh, M.V., Rahimpour-Bonab, H. 2007. Petrology and Geochemistry of the Granitoid Complex of Boroujerd, Sanandaj-Sirjan Zone, Western Iran. *Journal of Asian Earth Sciences*, 29: 859- 877.
- London, D., Morgan, G.B., Wolf, D. 1996. Boron in granitic rocks and their contact aureoles. In: Grew ES, Anovitz LM (eds) Boron. *Mineralogy, Petrology and Geochemistry*. The Mineralogical Society of America, Washington, DC, *Reviews in Mineralogy*, 33: 299-330.
- London D., Manning D.A.C., 1995. Chemical variation and significance of tourmaline from SW England. *Economic Geology*, 90, 495- 519.
- Manning, D.A.C., 1982. Chemical and morphological variation in tourmalines from the Hub Kapong batholith of Peninsular Thailand. *Mineralogical Magazine*, 45, 139-147.
- Masoudi, F., 1997. Contact metamorphism and pegmatite development in the region of SW Arak, Iran. PhD Thesis, Leeds University, UK.
- Mohajjel, M., Fergusson, C.L., Sahandi, M.R. 2003. Cretaceous–Tertiary convergence and continental collision, Sanandaj-Sirjan Zone, Western Iran. *Journal of Asian Earth Sciences*, 21: 397–412.
- Morgan, G.B., London, D., 1989. Experimental reactions of amphibolite with boron-bearing aqueous fluids at 200 MPa: Implications for tourmaline stability and partial melting in mafic rocks. *Contributions to Mineralogy and Petrology*, 102: 281-297.
- Nekouvaght, Tak, M.A., Bazargani-Guilani, K., 2009. Chemical Variation of Tourmaline and Source of Hydrothermal Solutions in Nezam Abad W-(Sn) Ore Deposit, Sanandaj-Sirjan Zone, West-Central Iran. *Journal of Sciences, Islamic Republic of Iran*, 20(2): 115-126.

- Nicholson, P.M., 1980. The geology and economic significance of the Golden Dyke dome, Northern Territory. In: J. Ferguson, A.B. Goleby eds Uranium in the Pine Creek Geosyncline. Int'l Atomic Energy Agency, Vienna, 319-334.
- Raith, J.G., Riemer, N., Meisel, S.T., 2004. Boron metasomatism and behavior of rare earth elements during formation of tourmaline rocks in the eastern Arunta Inlier, central Australia. *Contribution to Mineralogy and Petrology*, 147: 91–109.
- Slack, J.F., 1982. Tourmaline in Appalachian-Caledonian massive sulphide deposits and its exploration significance. *Trans Inst Min Metal* 91b, B81-B89.
- Sun, S.S., McDonough, W.F., 1989. Chemical and isotopic systematics of the oceanic basalts: implications for mantle composition and processes: in Saunders, A.D., Norry, M.J., (Eds.), *Magmatism in the Oceanic Basalts*. Geological Society of London, Special Publications, 42: 313-345.
- Wolf, M.B., London, D., 1997. Boron in granitic magmas: stability of tourmaline in equilibrium with biotite and cordierite. *Contribution to Mineralogy and Petrology*, 130:12-30.
- Yavuz, F., Yavuz, V., Sasmaz, A., 2006. WinClastour –A visual basic program for tourmaline formula recalculation and classification. *Computers and Geosciences*, 32: 1156-1168.